Low energy single pion production processes $\pi N \to \pi \pi N$

T. S. Jensen and A. F. Miranda

Institute of Physics and Astronomy, Aarhus University, DK-8000 Aarhus C, Denmark

(Received 9 May 1996)

Using baryon chiral perturbation theory (BχPTh), explicitly including the $\Delta(1232)$ and $N^*(1440)$ baryon resonances only, we compute for incoming $\pi^\pm P$ channels with kinetic energy under 400 MeV, total cross sections, angular distributions, and various final state correlation functions and compare these with available experimental data in this energy range. Threshold isospin amplitudes are extracted from the calculated fully covariant perturbative amplitudes. No attempt is made to fit this data. The necessary input parameters were all taken from separate experimental data. The results appear to be generally encouraging for BχPTh. [S0556-2813(97)00502-5]

I. INTRODUCTION

The subject of pionic interactions was for many years and still is the focus of much theoretical and experimental attention. Laboratory results on single pion production off nucleon targets via π and γ probes do provide some indirect evidence of the fundamental $\pi\pi$ interaction. On the other hand, these production processes certainly have intrinsic interest. Both the quantity and improving quality of the experimental data justify the continuing efforts to find a proper theoretical analysis and more detailed understanding of such processes.

This paper is a contribution to the ongoing effort to understand in particular the dynamics underlying the $\pi N \to \pi\pi N$ production reactions. Baryon chiral perturbation theory (BχPTh) is supposed to be a reliable theoretical instrument for analysis at very low energies above thresholds. We use it here, but phenomenologically motivated assumptions are added whenever deemed necessary, within a strictly covariant formalism. We do not attempt any fittings of observables: all the necessary input parameters are extracted from separate experimental and theoretical results.

Section II defines conventions and establishes the kinematics of the processes considered; Sec. III explains the basic theory and all the necessary approximations made, together with phenomenological input. Section IV presents and discusses our results and confronts these with the available experimental information.

II. CONVENTIONS, DEFINITIONS, KINEMATICS

Figure 1 represents the set of single-pion production processes studied in this paper (Table I). The kinematic variables are shown in Fig. 1 (we use Bjorken and Drell conventions [1]). We define

$$s = (p_1 + k_1)^2 = (p_2 + k_2 + k_3)^2 \tag{2.1}$$

and

$$T_{\pi_1} = \sqrt{|\mathbf{k}_1|^2 + m_1^2} - m_1. \tag{2.2}$$

as the kinetic energy of the incoming pion. The rest masses of pions are $m_i (i=1,2,3)$ and of nucleons are $M_i (i=1,2)$. Quantities referring to the center of mass (CM) system are labelled c.m.

The values for the physical parameters used are taken from Ref. [2]. At threshold, the pion kinetic energy in the LAB system is

$$T_{\pi_1 \text{th}} = \frac{s_{\text{th}} - m_1^2 - M_1^2}{2M_1} - m_1. \tag{2.3}$$

Table I shows its values for all five reactions considered. The following observables were computed: (1) Total cross sections for pion kinetic energies up to about 400 MeV; (2) Differential cross sections and angular correlation function for the experimentally well-studied reaction $\pi^- p \to \pi^+ \pi^- n$; (3) Invariant mass distributions for the final pion pair ($\pi^\circ \pi^\circ$) in reaction $\pi^- p \to \pi^\circ \pi^\circ n$ and ($\pi^- n$), ($\pi^+ n$) mass distributions for the reaction $\pi^- p \to \pi^+ \pi^- n$.

The cross section is given by

$$\sigma = \frac{(2\pi)^4 S}{2\lambda^{1/2}(s, m_1^2, M_{n_1}^2)} \int \cdots \int \delta^{(4)}(p_1 + k_1 - p_2 - k_2 - k_3)$$

$$\times \overline{|M_{\text{sr}}|^2} \frac{d^3\mathbf{p}_2}{(2\pi)^3 2E_{n_2}} \frac{d^3\mathbf{k}_2}{(2\pi)^3 2w_2} \frac{d^3\mathbf{k}_3}{(2\pi)^3 2w_3}, \tag{2.4}$$
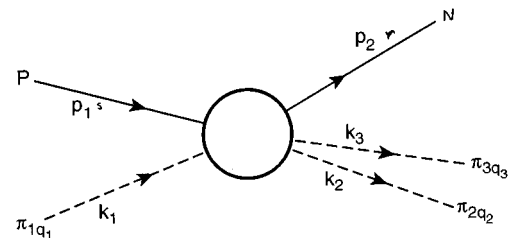

FIG. 1. Kinematic variables for reactions I—V (Table I). p_i and k_i are four-momenta of baryons and pions, respectively; q_i denote the third isospin component of particle i; s and r are polarizations of the incoming and outgoing nucleons, respectively.

TABLE I. The third column gives the incoming pion LAB kinetic energy in MeV at threshold; the last column gives the value of the total isospin component I_3. Reaction I and II thus involve only $2I=3$ whereas the remaining ones involve both $2I=3$ and $2I=1$.

	Reaction	$T_{\pi_1 \text{th LAB}}$ (MeV)	$2I_3$
I	$\pi^+ p \rightarrow \pi^+ \pi^+ n$	172.387	3
II	$\pi^+ p \rightarrow \pi^+ \pi^\circ p$	164.759	3
III	$\pi^- p \rightarrow \pi^+ \pi^- n$	172.587	-1
IV	$\pi^- p \rightarrow \pi^\circ \pi^\circ n$	160.499	-1
V	$\pi^- p \rightarrow \pi^\circ \pi^- p$	164.759	-1

where S is a symmetry factor equal to 1/2 for identical final pions, 1 otherwise. λ is the Källen function,

$$\lambda(x,y,z) = x^2 + y^2 + z^2 - 2(xy + xz + yz). \quad (2.5)$$

E_{n_2}, w_2, and w_3, respectively, are the final nucleon energy, and the energies of pion 2 and pion 3.

The main subject of this paper is M_{sr}, the invariant Feynman amplitude for the process. As we do not consider polarization experiments in this paper, the usual statistical averaging is performed upon σ_{sr}. The calculation of M_{sr} is the topic of Sec. III; all calculations were performed with the help of an extended version of the computer code PHYSICA, a MATHEMATICA package initially created by Beringer [3]. The actual expression for M_{sr} is unfortunately too involved to be reproduced here, but we hope that the many detailed figures shown may compensate for this.

III. BASIC THEORY AND APPROXIMATIONS

A. Propagators and vertices

BχPTh underlies all calculations reported in this paper [3–7].

The Lagrangian density is split into quadratic and nonquadratic (interaction) terms:

$$\mathcal{L} = \mathcal{L}_{\text{quad}} + \mathcal{L}_{\text{int}}. \quad (3.1)$$

The quadratic part includes an isospin 1 massive pseudoscalar (pion π), two massive isodoublets, spin-1/2 baryons [N and $N^*(1440)$] and a massive isoquadruplet, spin-3/2 baryon [$\Delta(1232)$]. No heavy meson resonances were explicitly included. The "interaction" part of the Lagrangian is written according to the rules of BχPTh [3–6]. We then compute the leading order Feynman diagrams shown in Fig. 2, using PHYSICA, as mentioned.

The couplings actually considered contain at most two derivatives of the pion field. Each allowed term is expanded in powers of the pion field. Thus we get, keeping at most four pions,

$$\mathcal{L}_{\text{int}} = \mathcal{L}_{\pi\pi\pi\pi} + \mathcal{L}_{NN\pi} + \mathcal{L}_{NN\pi\pi} + \mathcal{L}_{NN\pi\pi\pi} + \cdots + \mathcal{L}_{N\Delta\pi}$$
$$+ \mathcal{L}_{N^*N\pi} + \cdots. \quad (3.2)$$

The interaction terms shown below are given in the σ-gauge [5], but as it is well known, the S-matrix elements
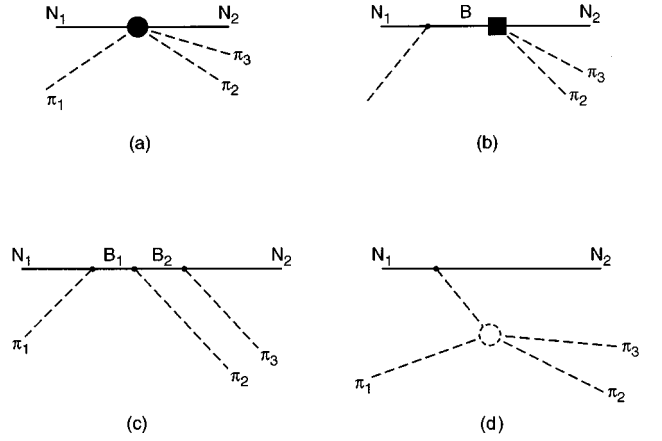

FIG. 2. Feynman diagrams for the leading order amplitudes calculated in this paper. Physical masses for all particles are used. Only intermediate baryons N, N^* and Δ were actually included: (b) $B = N, N^*$; (c) $(B_1, B_2) = (\Delta, N) + (N, \Delta)$. Vertex (d) includes only the leading order (Weinberg) $\pi\pi$ interaction.

of interest are independent of the field parametrization. All parameters appearing in this Lagrangian will be discussed in Sec. IV.

1. Pion self-couplings

This is given by the first term in Eq. (3.2):

$$\mathcal{L}_{\pi\pi\pi\pi} = \frac{1}{8F^2}[(\partial\boldsymbol{\pi}^2)^2 - m_\pi^2 \boldsymbol{\pi}^4]. \quad (3.3)$$

2. Nucleon-pion couplings

These are given by the next three terms in Eq. (3.2):

$$\mathcal{L}_{NN\pi} = -\frac{g_A}{2F} \bar{N} \gamma^\mu \gamma_5 \boldsymbol{\tau} \cdot \partial_\mu \boldsymbol{\pi} N, \quad (3.4a)$$

$$\mathcal{L}_{NN\pi\pi} = -\frac{1}{4F^2} \bar{N} \gamma^\mu \boldsymbol{\tau} \cdot (\boldsymbol{\pi} \times \partial_\mu \boldsymbol{\pi}) N, \quad (3.4b)$$

$$\mathcal{L}_{NN\pi\pi\pi} = -\frac{g_A}{8F^3} \bar{N} \gamma^\mu \gamma_5 \boldsymbol{\tau} \cdot \boldsymbol{\pi} \partial_\mu \boldsymbol{\pi}^2 N. \quad (3.4c)$$

3. NΔ-pion coupling

The Δ multiplet is strongly coupled to the π-N system and lies too close to our thresholds to be ignored. Its width is such that it plays a very important role in the threshold energy region that we are especially interested in. For the Δ we use the Rarita-Schwinger representation for the field [8]. Then the corresponding quadratic part of the Lagrangian is

$$\mathcal{L}_\Delta = \bar{\Psi}^\mu \Lambda_{\mu\nu} \Psi^\nu \quad (3.5)$$

with

$$\Lambda_{\mu\nu} = (-i\not{\partial} + M_\Delta)g_{\mu\nu} - iA(\gamma_\mu \partial_\nu + \gamma_\nu \partial_\mu)$$

$$-\frac{i}{2}(3A^2 + 2A + 1)\gamma_\mu \not{\partial} \gamma_\nu$$

$$- M_\Delta(3A^2 + 3A + 1)\gamma_\mu \gamma_\nu, \qquad (3.6)$$

where $A(\neq -1/2)$ was taken to be an arbitrary (real) constant. We chose $A = -1$, in which case the momentum space Δ propagator to be used in the Feynman rules becomes $-iS_{\mu\nu}(p)$ with

$$S_{\mu\nu}(p) = \frac{\not{P} + M_\Delta}{p^2 - M_\Delta^2}\left(g_{\mu\nu} - \frac{1}{3}\gamma_\mu \gamma_\nu - \frac{2p_\mu p_\nu}{3M_\Delta^2}\right.$$

$$\left. + \frac{p_\mu \gamma_\nu - p_\nu \gamma_\mu}{3M_\Delta}\right). \qquad (3.7)$$

The interaction term for $\Delta - \pi$ that we considered is linear in the pion field:

$$\mathcal{L}_{N\Delta\pi} = -\frac{g_\Delta}{2F}\overline{\Delta}_\mu T^a\left[g^{\mu\nu} - \left(Z + \frac{1}{2}\right)\gamma^\mu \gamma^\nu\right] \qquad (3.8)$$

$$\times \partial_\nu \pi^a N + \text{H.c.} \qquad (3.9)$$

where Δ_μ is now the Rarita-Schwinger field with the propagator $-iS_{\mu\nu}(p)$; $T^a(a=1,2,3)$ are transition isospin matrices; Z is a parameter [9]. There is some uncertainty about its numerical value, but within a reasonable range (see Sec. IV) our result turns out not to be too sensitive to its exact value. We note in passing that this Z appears to be irrelevant for nonrelativistic, or static model, approximations. In computing amplitudes, naive use of Eq. (3.7) would be dangerous, of course, as the Δ width [2] (≈ 120 MeV) is comparable to the energy range above threshold for which the theory we are sketching here is supposed to be reliable. We then follow the usual procedure [10–15], i.e., we modify the propagator so that

$$\frac{1}{p^2 - M_\Delta^2} \to \frac{1}{p^2 - M_\Delta^2 + i\Gamma_\Delta(\sqrt{s})M_\Delta}. \qquad (3.10)$$

The dependence of the Δ width on its c.m. energy $\sqrt{s}$ can be parameterized in many ways. We return to this question in Sec. IV.

4. NN*-coupling to pions

The Roper resonance [2] $N^*(1440)$ lies too close to our target area of interest. Moreover, it does couple with appreciable strength to specific subchannels [2] such as $N^* \to N(\pi\pi)_{I=0}$. We therefore explicitly included it as we should expect sensitivity of our results to its presence and properties. We thus must add further contributions to our effective Lagrangian in the form permitted by BχPTh [3–6]:

$$\mathcal{L}_{N^*N\pi} = -\frac{g_{N^*}}{2F}\overline{N}^*\boldsymbol{\tau}\cdot\partial_\mu \boldsymbol{\pi}\gamma^\mu \gamma_5 N + \text{H.c.} \qquad (3.11)$$

and

$$\mathcal{L}_{N^*N\pi\pi} = \frac{1}{F^2}\overline{N}^*[-C_1^* m_\pi^2 \boldsymbol{\pi}^2 + C_3^*(\partial_\mu \boldsymbol{\pi})^2]N + \text{H.c.} \qquad (3.12)$$

We thus introduce three further phenomenological parameters, viz., g_{N^*}, C_1^*, and C_3^*. Unfortunately, we are now reaching the limits that allow us more or less precise extraction of individual parameters from relevant experimental results. As we shall see in the next section, only a certain polynomial in C_1^* and C_3^* can be (roughly) fixed by the available data.

Like the Δ, the N^* linewidth is also too large (from our point of view) not to warrant explicit inclusion. We use the same recipe as for the Δ, i.e., we modify its propagator

$$\frac{1}{p^2 - M_{N^*}^2} \to \frac{1}{p^2 - M_{N^*}^2 + i\Gamma_{N^*}(\sqrt{s})M_{N^*}}. \qquad (3.13)$$

We discuss the importance of energy dependence of Γ_{N^*} in the following section.

Having thus defined the vertices and propagators, PHYSICA straightforwardly computes the tree diagrams of the type shown in Fig. 2. The resulting amplitude can be put in the form

$$M_{\text{sr}} = \overline{u}_{p_2 r}\gamma_5[f_1 + f_2\not{k}_2 + f_3\not{k}_3 + f_4\not{k}_2\not{k}_3]u_{p_1 s}, \qquad (3.14)$$

where $\overline{u}_{p_2 r}$ and $u_{p_1 s}$, respectively, are Dirac spinors for the final and the initial nucleon; in our PHYSICA computer program they are normalized as $\overline{u}_r(\mathbf{p})u_s(\mathbf{p}) = 2M\delta_{rs}$, where M is the proton mass. The $f_i(i=1,\ldots,4)$ are Lorentz scalar functions of the four-scalar products constructed with the incoming and outgoing four-momenta, due account being taken, of course, of four-momentum conservation and that all particles are on their mass shells. They are calculated by PHYSICA [3].

B. Very low-energy amplitudes

The single pion production off nucleon targets has a special interest in the context of BχPTh, as these processes do provide indirect evidence concerning the basic π-π interaction near threshold. We can easily extract from our results on the Lorentz invariant amplitudes some relevant numbers giving our threshold values for these amplitudes. We show only typical values at thresholds of these amplitudes that lead to a reasonable overall description of all available data up to few tens of MeV above thresholds (Table II). In order to facilitate comparison with other authors, we define $M_{\text{sr}} \equiv A_{\text{sr}}2M$, where the Dirac spinors in A_{sr} have the Bjorken-Drell normalization $\overline{u}_s(\mathbf{p})u_r(\mathbf{p}) = \delta_{\text{sr}}$.

In the CM system, with all momenta close to threshold, this boils down to

$$A_{\text{sr}} = a\chi_r^+ \mathbf{k}_{1\text{c.m.}}\cdot\boldsymbol{\sigma}\chi_s + b\chi_r^+ \mathbf{k}_{23}\cdot\boldsymbol{\sigma}\chi_s + c\chi_r^+ \mathbf{K}_{23}\cdot\boldsymbol{\sigma}\chi_s + \cdots, \qquad (3.15)$$

where $\mathbf{k}_{1\text{c.m.}}$ is the three-momentum of the incoming pion and

TABLE II. Numerical values at threshold $F_i \equiv (f_i)_{thr}(i=1,\ldots,4)$ for each of the five processes listed in Table I. These threshold values are made dimensionless by multiplying into appropriate powers of $m_\pi = 139.5679$ MeV. Parameters fixed at: $F = 93$ MeV; $g_A = 1.327$; $g_D = 2.81$, $Z = -1/2$; $M_P = M_N = 938.27231$ MeV; $m_{\pi^\pm} = m_{\pi^\circ} = 139.56955$ MeV; $M_\Delta = 1232$ MeV; $M_{N*} = 1440$ MeV; $\bar{c}_1^* = -0.76 \bar{c}_3^* = 0$.

Reaction	$\mathrm{Re}F_1 \times m_\pi^{-2}$	$\mathrm{Im}F_1 \times m_\pi^{-2}$	$\mathrm{Re}F_2 \times m_\pi^{-3}$	$\mathrm{Im}F_2 \times m_\pi^{-3}$	$\mathrm{Re}F_3 \times m_\pi^{-3}$	$\mathrm{Im}F_3 \times m_\pi^{-3}$	$\mathrm{Re}F_4 \times m_\pi^{-4}$	$\mathrm{Im}F_4 \times m_\pi^{-4}$
I	0.72	22.35	0.42	−1.50	0.42	−1.50	0	0
II	42.16	2.48	42.24	16.31	−43.15	−13.92	−43.69	−13.52
III	−19.88	−90.85	−19.86	−32.10	19.78	39.72	20.00	38.37
IV	−1.18	58.10	0.35	−6.60	0.33	−6.60	0	0
V	14.39	−36.84	14.24	−25.58	−13.94	28.46	−14.14	25.83

$$\mathbf{k}_{23} \equiv \mathbf{k}_{2\mathrm{c.m.}} - \mathbf{k}_{3\mathrm{c.m.}},$$

$$K_{23} = \mathbf{k}_{2\mathrm{c.m.}} + \mathbf{k}_{3\mathrm{c.m.}} \tag{3.16}$$

with χ_r, χ_s and σ being (spin) Pauli spinors and Pauli matrices, respectively.

For each process

$$a = \frac{1}{2M}[(F_2 + F_3)m_\pi - F_1 - m_\pi^2 F_4],$$

$$b = \frac{1}{2}(F_2 - F_3 + 2m_\pi F_4),$$

$$c = \frac{1}{2}(F_2 + F_3), \tag{3.17}$$

where the F_i are threshold values of the f_i, M is the proton mass, and m_π is the $\pi^\pm$ mass. Exactly at threshold, the b and c terms in Eq. (3.15) do not contribute, of course. In computing these amplitudes, exact isospin invariance was assumed. Thus ignoring the actual mass splittings within the isotriplet and the baryonic isomultiplets we can easily determine the isospin amplitudes at and near threshold. The isospin channels involved are $I = 3/2$ and $I = 1/2$; the two pions in the final state can be in $I_{23} = 0,2$ states or $I_{23} = 1$ state, associated with relative S and P waves in the overall CM system, respectively, according to the Bose symmetry. From the above, it is clear that only amplitudes of S waves contribute at threshold through $A^{2I,I_{23}} = A^{32}$ and A^{10}. In general, we have in obvious notation

$$A_{q_{n_1} q_{n_2}}^{q_1 q_2 q_3} = \sum_I \sum_{I_{23}} \left(1 q_1 \frac{1}{2} q_{n_1} \middle| IQ \right)(1 q_2 1 q_3 | I_{23} Q_{23})$$

$$\times \left(I_{23} Q_{23} \frac{1}{2} q_{n_2} \middle| IQ \right) A^{2I,I_{23}}. \tag{3.18}$$

We have suppressed all non-isospin-related labels. We must have, of course, $q_1 + q_{n_1} = q_2 + q_3 + q_{n_2} = Q$, but total isospin invariance ensures that the $A^{2I,I_{23}}$ are independent of Q.

Inserting Eq. (3.17) into Eq. (3.18) we get, in obvious notation,

$$a^{32} = \frac{\sqrt{5}}{2}a^I,$$

$$a^{10} = \frac{3}{\sqrt{2}}a^{IV} - \frac{1}{\sqrt{2}}a^I \tag{3.19}$$

and similarly for $b^{2I,I_{23}}$ and $c^{2I,I_{23}}$. The relevant threshold isospin amplitudes are thus a^{32} and a^{10}. Very close to threshold b^{31}, b^{11}, c^{31}, and c^{11} contribute as well, according to Eq. (3.15). Table II shows representative results for the threshold values that we calculated for the four amplitudes f_1, f_2, f_3, and f_4 for each of the five reactions considered in this paper.

IV. RESULTS, DISCUSSION, AND CONCLUSION

In calculating the amplitudes corresponding to the Feynman diagrams of Fig. 2 (except at threshold) we assumed physical masses for all particles involved [2]. We still have an additional nine parameters.

F, g_A, g_D, Z, Γ_Δ, Γ_{N*}, g_{N*}, C_1^*, and C_3^*, are to be fixed before we can compute observables.

We fixed the first four of these parameters to the values [3–7,9,10]

$$F = 93 \text{ MeV},$$

$$g_A = 1.327,$$

$$g_D = 2.81,$$

$$Z = -1/2. \tag{4.1}$$

The value for g_D was determined from the SU(4) relation [13]

$$g_D = \frac{3}{\sqrt{2}}g_A. \tag{4.2}$$

As to the off-shell parameter Z, there is, as mentioned earlier, some uncertainty about its appropriate value. However, it was established [9] that

$$-0.8 < Z < 0.3.$$

To check the sensitivity to Z we simply computed the amplitude for $\pi^- p \to \pi^+ \pi^- n$ for Z in this range and found

that our numerical results for the amplitude changed very little. We therefore fixed Z to $-1/2$, as this does speed up the numerical work considerably.

Next, we turn to the parameters Γ_Δ and Γ_{N*} which play an important role in our work. The importance of Γ_Δ can be immediately gleaned from the $\pi N \rightarrow \pi N$ data [2]. The energy dependence of Γ_Δ and Γ_{N*} is discussed in the literature [10–12,15]. We have tried the following recipes:

Γ_Δ *width.* There are three useful parametrizations:

$$\Gamma_\Delta(\sqrt{s}) \equiv \Gamma_1(\sqrt{s}) = \text{const}, \qquad (4.3a)$$

$$\Gamma_\Delta(\sqrt{s}) \equiv \Gamma_2(\sqrt{s}) \propto k^3/\sqrt{s} \qquad (4.3b)$$

$$\Gamma_\Delta(\sqrt{s}) \equiv \Gamma_3(\sqrt{s}) \propto \frac{k^3}{(k^2 - 0.024 \text{ GeV}^2)(k^2 - 0.04 \text{ GeV}^2)}, \qquad (4.3c)$$

where k and $\sqrt{s}$ are the magnitude of the pion three-momentum and energy of the Δ in the overall CM system, respectively. The condition [2]

$$\Gamma_\Delta(M_\Delta) = 120 \text{ MeV}$$

fixes the normalizations in Eq. (4.3). Thus the three expressions for Γ_Δ have a common value of 1232 MeV with this $\Gamma_\Delta(M_\Delta)$.

Γ_{N*} *width.* Again, we tried three different parametrizations:

$$\Gamma_{N*}(\sqrt{s}) \equiv \Gamma_1(\sqrt{s}) = \text{const}, \qquad (4.4a)$$

$$\Gamma_{N*}(\sqrt{s}) \equiv \Gamma_2(\sqrt{s}) \propto k^3, \qquad (4.4b)$$

$$\Gamma_{N*}(\sqrt{s}) \equiv \Gamma_3(\sqrt{s}) \propto \frac{k^3}{(k^2 - 0.025 \text{ GeV}^2)(k^2 - 0.09 \text{ GeV}^2)}. \qquad (4.4c)$$

Parametrization (4.4b) is similar to the one recommended in [12,15]. Note the differences between Eqs. (4.3b) and (4.4b). There is, however, only a very mild dependence on $\sqrt{s}$ in the energy region crucial to us. The experimental uncertainties on Γ_{N*} are not small, unfortunately; it is given that $\Gamma_{N*} = 250 - 450$ MeV [2]. From the branching ratio (BR) [2] for the $N* \rightarrow N\pi$ channel of about 60–70 % we deduce that the partial decay width is $\Gamma_{N*N\pi} \approx 228$ MeV, the value actually used in our final results which are shown in Figs. 3–8.

We thus obtained

$$g_{N*} = 0.63 \pm 0.11. \qquad (4.5)$$

The central value agrees with [15] and the uncertainty comes from the above-quoted uncertainty in the BR [2].

The determination of C_1^* and C_3^* follows along similar lines (see Appendix). We apply the effective interaction (3.12) to the decay channel

$$N* \rightarrow N(\pi\pi)_{I=0}$$

having the BR between 5% and 10% [1].

We thus find

$$\Gamma_{N(\pi\pi)_{I=0}} = \alpha C_1^{*2} + 2\beta C_1^* C_3^* + \gamma C_3^{*2}, \qquad (4.6)$$

where α, β, and γ are constants. This ellipse is discussed in the Appendix. The area between the stippled ellipses is the one allowed by the data. The central ellipse corresponds to the value

$$\Gamma_{N(\pi\pi)_{I=0}} = 26 \text{ MeV}. \qquad (4.7)$$

The $N*N\pi\pi$ vertex (represented by the parameters C_1^* and C_3^*) is especially significant for the processes $\pi^- p \rightarrow \pi^+ \pi^- n$ and $\pi^- p \rightarrow \pi^\circ \pi^\circ n$.

We first set $C_3^* = 0$ in agreement with Oset *et al.* [12], Sossi *et al.* [16]. This helped us in comparing our results with theirs, but we shall presently return to other options and in fact show how the $\pi N \rightarrow \pi\pi N$ data could help in producing useful bonds on these parameters.

Among the best available low-energy data [17] is the total cross section for $\pi^- p \rightarrow \pi^\circ \pi^\circ n$. The choice of C_1^* was then determined by using the Lowe and Burkardt [18] model independent fit (A) for this reaction at Lab momentum 310 MeV/c corresponding to an incoming pion kinetic energy of 200.4 MeV. At this energy, the total cross section is given as 18.1 μb. We chose C_1^* so that we match this number. Our amplitudes for $\pi N \rightarrow \pi\pi N$ turn out to depend only on the combination $g_{N*}C_{1,3}^*$. We therefore define the dimensionless constants

$$\bar{c}_{1,3}^* = g_{N*} m_\pi C_{1,3}^*/0.63 \qquad (4.8)$$

and use $\bar{c}_1^*, \bar{c}_3^*$ instead of C_1^*, C_3^*.

For the above-mentioned three different choices for Γ_Δ and Γ_{N*} we find

$$\Gamma = \Gamma_1 : \bar{c}_1^* = -1.09,$$

$$\Gamma = \Gamma_2 : \bar{c}_1^* = -0.76,$$

$$\Gamma = \Gamma_3 : \bar{c}_1^* = -0.86, \qquad (4.9)$$

which all agree with the quoted partial line width. We choose the sign of $\bar{c}_1^*$ to be negative in order to agree with the convention in expression (3.12).

The results turn out to be rather sensitive to Γ_{N*}. Unless otherwise stated, we present our result for the choice Γ_2.

We briefly discuss in the Appendix the consequences of having $\bar{c}_3^* \neq 0$ [19]. In Figs. 9(a) and 9(b) we show the results for $\bar{c}_1^* = -0.37$, $\bar{c}_3^* = -0.20$ (preferred parameters if an energy dependent Γ is chosen). $\bar{c}_1^* = -0.72$, $\bar{c}_3^* = -0.09$, preferred parameters if an energy independent Γ is chosen.

Müller *et al.* [20] measured the correlation function $W(\pi^-)$ for $\pi^- p \rightarrow \pi^+ \pi^- n$:

$$W(\pi^-) = 4\pi \frac{d^3\sigma}{d\Omega_2 dk_2 d\Omega_3} \bigg/ \frac{d^2\sigma}{d\Omega_2 dk_2}, \qquad (4.10)$$

where k_2 is the magnitude of the three-momentum of final π^- in the center of mass system and $\Omega_2(\Omega_3)$ is the solid angle subtended by $\pi^-(\pi^+)$ in the final state. The probability distribution $W(\pi^-)$ is normalized to 1 for an isotropic π^- emission.
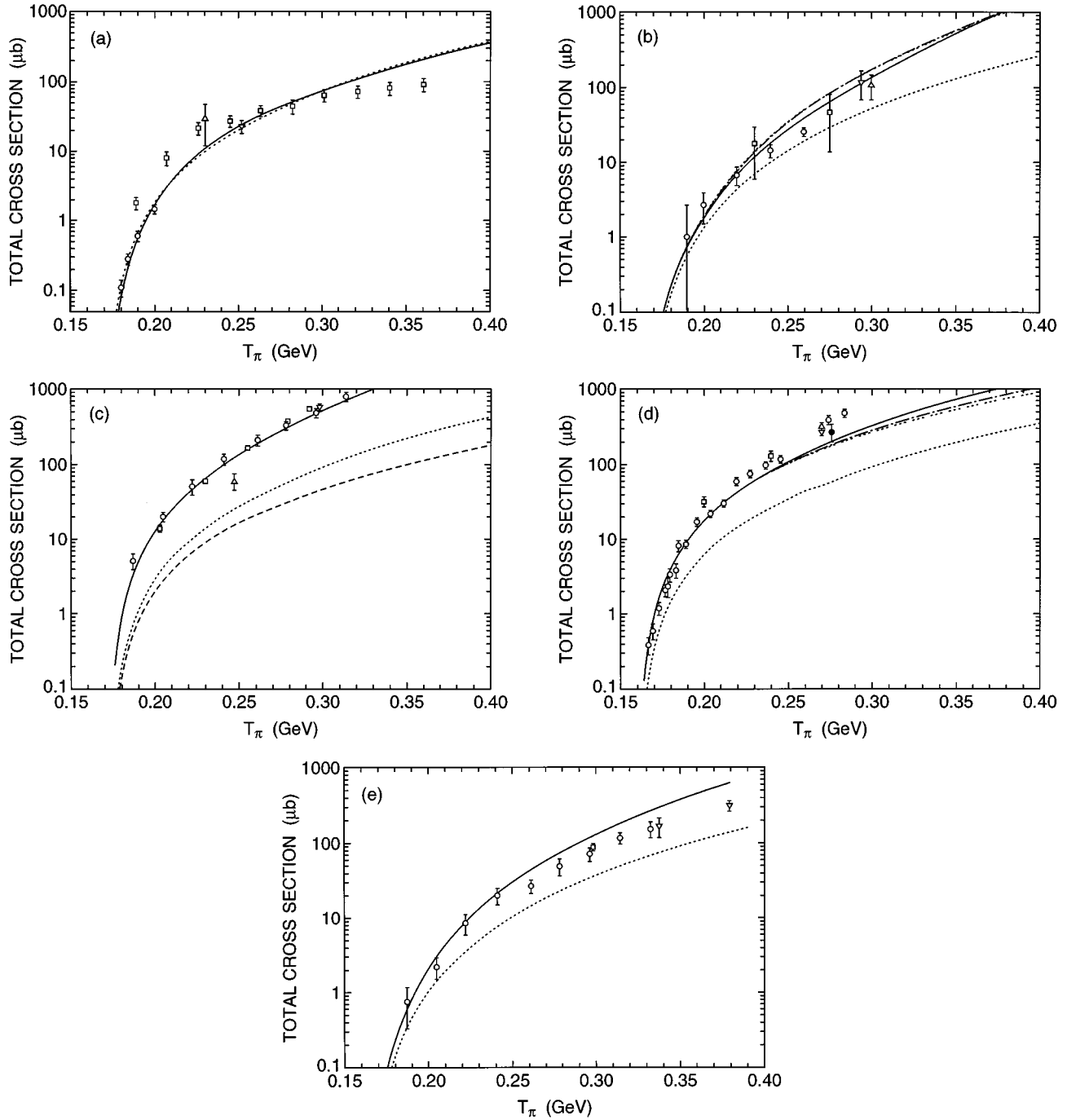
FIG. 3. Total reaction cross section for the various channels (a) I: —— with Δ and N^*; - - - - without Δ and N^*; $\bigcirc$ [29];$\square$ [24]; $\triangledown$ [30]; $\triangle$ [31]; (b) II: - - - - - - with $\Gamma=\Gamma_1$;—— $\Gamma=\Gamma_2$; — · — · — · $\Gamma=\Gamma_3$; - - - - - without Δ and N^*; $\bigcirc$ [22]; $\square$ [31]; $\triangledown$ [32]; $\triangle$ [33]; (c) III: —— with Δ and N^*; · · · · · · without Δ and N^*; - - - - $3\pi+4\pi$; $\bigcirc$ [25]; $\square$ [34]; $\triangledown$ [27]; $\triangle$ [35]; (d) IV: $\bigcirc$ [17]; $\square$ [36]; $\triangledown$ [37]; $\triangle$ [38]; $\bullet$ [30]; - - - - - - $\Gamma=\Gamma_1$; —— $\Gamma=\Gamma_2$; — · — · — · $\Gamma=\Gamma_3$. The Γ's are the three choices for the linewidths in the phenomenological expressions for the Δ and N^* propagators (Sec. IV); (e) V: —— with Δ and N^*; - - - - without Δ and N^*; $\bigcirc$ [25]; $\square$ [27]; $\triangledown$ [39].

The measurements were performed at 284 MeV, with the outgoing pion momenta between 37 and 174 MeV/c. As shown in [20] the results for W may deviate considerably from simple phase space distributions, which make them interesting for us. Unfortunately, we cannot expect the theory sketched out here to be at its best in the energy region investigated by Müller *et al.* Our numerical results [Figs. 7(a)–7(d)] confirm this expectation: agreement with the published results is generally poor for nearly all of the kinematic con-

figurations reported on, even with the full inclusion of both Δ and N^* and/or reasonable variation of some of the key parameters discussed in this paper. We believe that a better test of the BχPTh capacity in predicting these distributions could be obtained at energies somewhat closer to thresholds or perhaps with selected polarization measurements.

We return to our results for the threshold amplitudes, summarized in Table II. Other authors, e.g., [13], [21], and [22], have also given their attention especially to the isospin
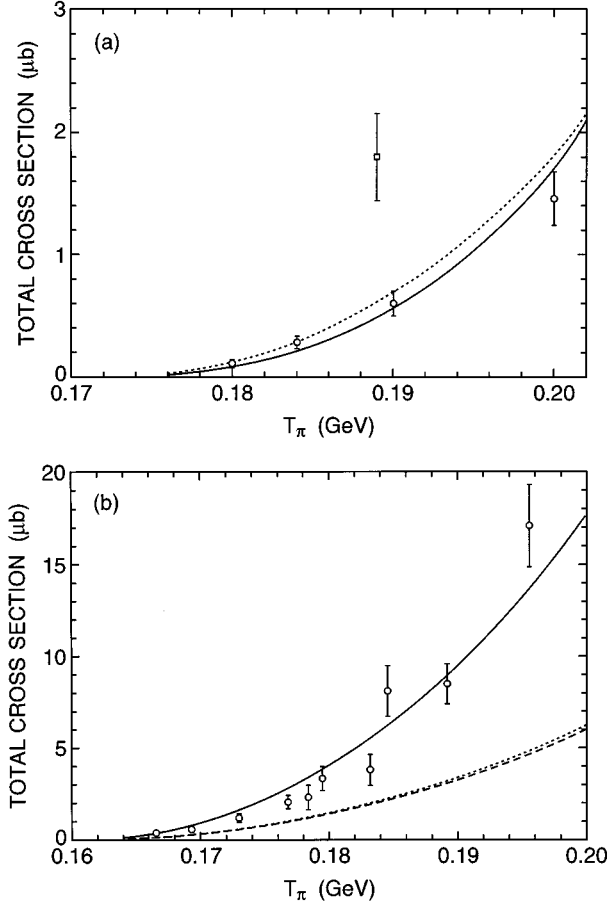
FIG. 4. Total reaction cross sections below about $T_\pi = 200$ MeV for channel I: (a) I: —— with Δ and N^*; - - - - without Δ and N^*; $\bigcirc$ [29]; $\square$ [24]; for channel IV: (b) —— with Δ and N^*; - - - - with Δ; $\cdots\cdots$ without Δ and N^*; $\bigcirc$ [17].

FIG. 5. Total reaction cross sections for (a) channel IV: —— $(\overline{c}_1^*, \overline{c}_3^*) = (-0.37, -0.20)$; - - - - $(\overline{c}_1^*, \overline{c}_3^*) = (-1.50, 0.70)$; $\bigcirc$ [17]; $\square$ [36]; $\triangledown$ [37]; $\triangle$ [38]; $\bullet$ [30]; (b) channel III: $\bigcirc$ [25], $\square$ [34], $\triangledown$ [27], $\triangle$ [35].

threshold amplitudes. Burkhardt and Lowe (BL) [21] extract these amplitudes from elaborate fits to the total cross sections (see their Fig. 1). One of their fits, carried out by assuming the constraints of the Olsson-Turner chiral-symmetry breaking model (fit B) leads to the results given in their Table I. They drop possible terms corresponding to our c_{31}, and c_{11}, as they neglect the three-momentum of the outgoing nucleon. We should recall that at the time BL did their work, the available data in the $\pi^+ \pi^0 p$ channel below 300 MeV was scarce and of too low accuracy to constrain their global fit. The analysis was furthermore complicated by inconsistencies in the published cross sections for the $\pi^+ \pi^+ n$ channel. Their amplitudes A_{32}, A_{10}, A_{31}, and A_{11} should correspond to our a^{32}, a^{10}, b^{31}, and b^{11}. We quote

$$A_{32} = 2.07 \pm 0.10,$$

$$A_{10} = 6.55 \pm 0.16,$$

$$A_{31} = -5.0 \pm 2.2,$$

$$A_{11} = 3.3 \pm 0.8.$$

Bernard, Kaiser, and Meissner (BKM) [23] have recently made a detailed theoretical analysis of these threshold iso-
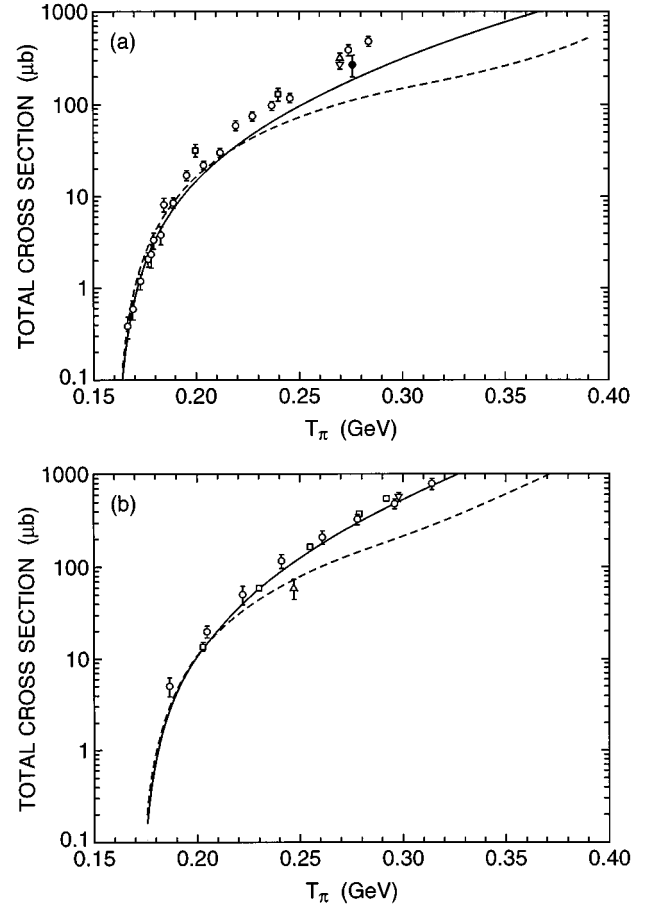
spin amplitudes. They define D_1 and D_2 related to the more commonly used amplitudes $A_{2I, I_{\pi\pi}}$ by the equations

$$D_1 = \frac{1}{\sqrt{10}} A_{32},$$

$$D_2 = -\frac{2}{3} \frac{A_{32}}{\sqrt{10}} - \frac{1}{3} A_{10}.$$

They predict, to order m_π^2,

$$D_1 = 2.65 \pm 0.24 F m^3,$$

$$D_2 = -9.06 \pm 1.05 F m^3.$$

Translating this to our units, we get

$$A_{32} = 2.96 \pm 0.08,$$

$$A_{10} = 7.74 \pm 1.28,$$

in units of m_π^{-3}. Using the results quoted in Table II we deduce
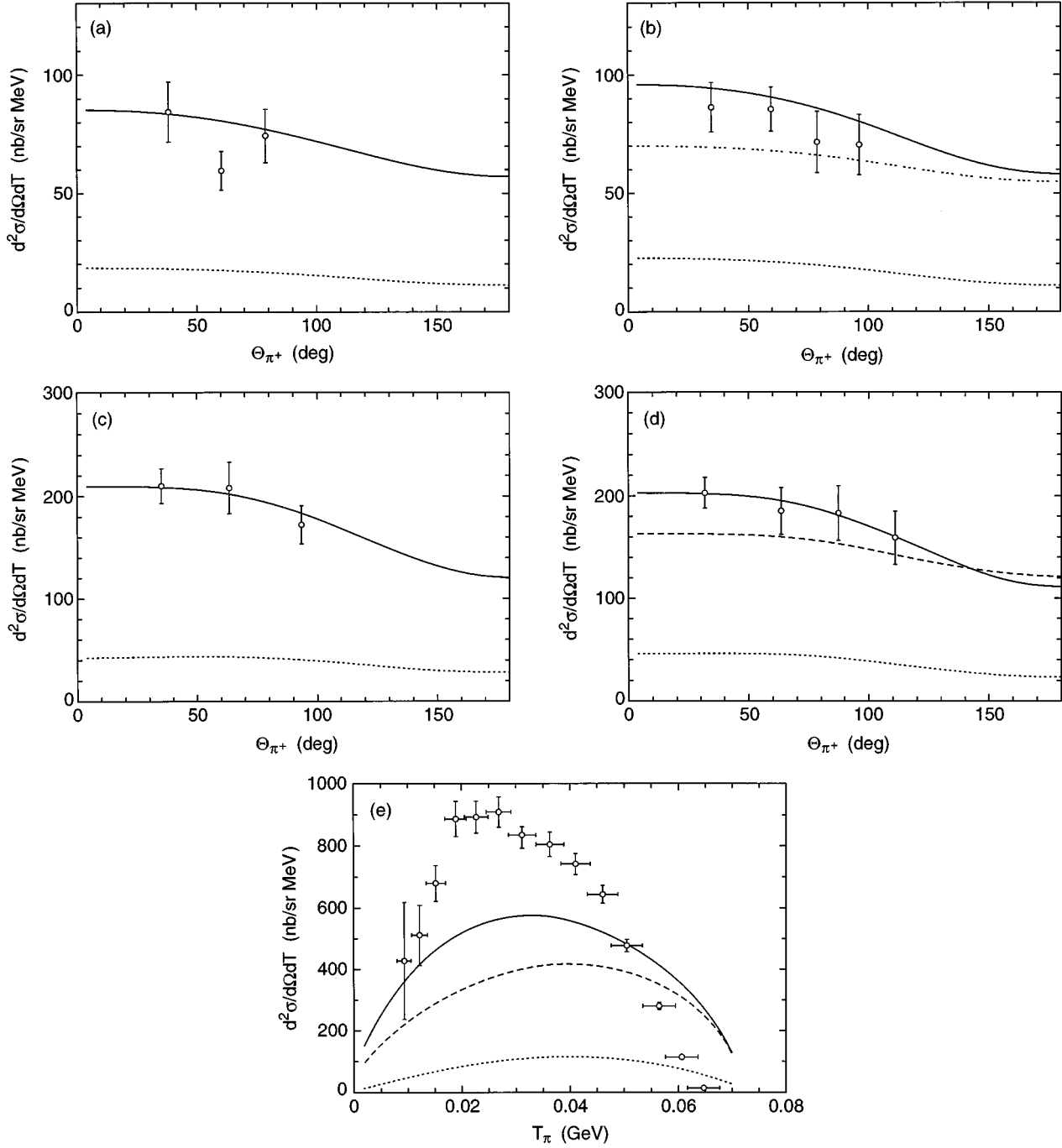
$$a^{32} = 2.10,$$

$$a^{10} = 9.92.$$

FIG. 6. The differential cross section III at 203 MeV [(a) and (b)], at 230 MeV [(c) and (d)] as functions of the outgoing pion π^+ kinetic energy T_{π^+}; θ_{π^+} is the angle between the direction of the incoming π^- momentum and the outgoing π^+ momentum in the center-of-mass frame: (a) T_{π^+} = 6.5 MeV; —— with Δ and N^*; - - - - without Δ and N^*; $\bigcirc$ [28]; (b) T_{π^+} = 11.0 MeV; —— with Δ and N^*; - - - - - - with N^*; - - - - - - without Δ and N^*; $\bigcirc$ [28]; (c): T_{π^+} = 17.5 MeV; —— with Δ and N^*; - - - - - without Δ and N^* $\bigcirc$ [28]; (d) T_{π^+} = 24.6 MeV; —— with Δ and N^*; - - - - with N^*; · · · · · · without Δ and N^*; $\bigcirc$ [28]. (e) The same, at 284 MeV and $\cos\theta_{\pi^+}$ = 0.174; the experimental data is given for $\cos\theta_+$ = 0.03—0.35, but the calculated cross section changes little as θ_{π^+} varies in this range; —— with Δ and N^*; - - - - with N^*; · · · · · · without Δ and N^*; $\bigcirc$ [20].

We thus all more or less disagree as to the central values of a^{32} and a^{10}. Nevertheless, we emphasize that our values for these quantities are consistent with our cross sections, which rather agree with the experimental data in the relevant energy range. Our results for a^{10} are very sensitive to the assumed properties for N^*, through the very important channel IV. By

small readjustments of $(\overline{c}_1^*, \overline{c}_3^*)$ inside the allowed elliptical band (Fig. 9) we could, however, reproduce the BL results. Unfortunately, that would impair the quality of our results for Reaction III.

We cannot, however, reproduce BKM's results for A^{32} by merely readjusting $(\overline{c}_1^*, \overline{c}_3^*)$ within the allowed band (Fig. 9).
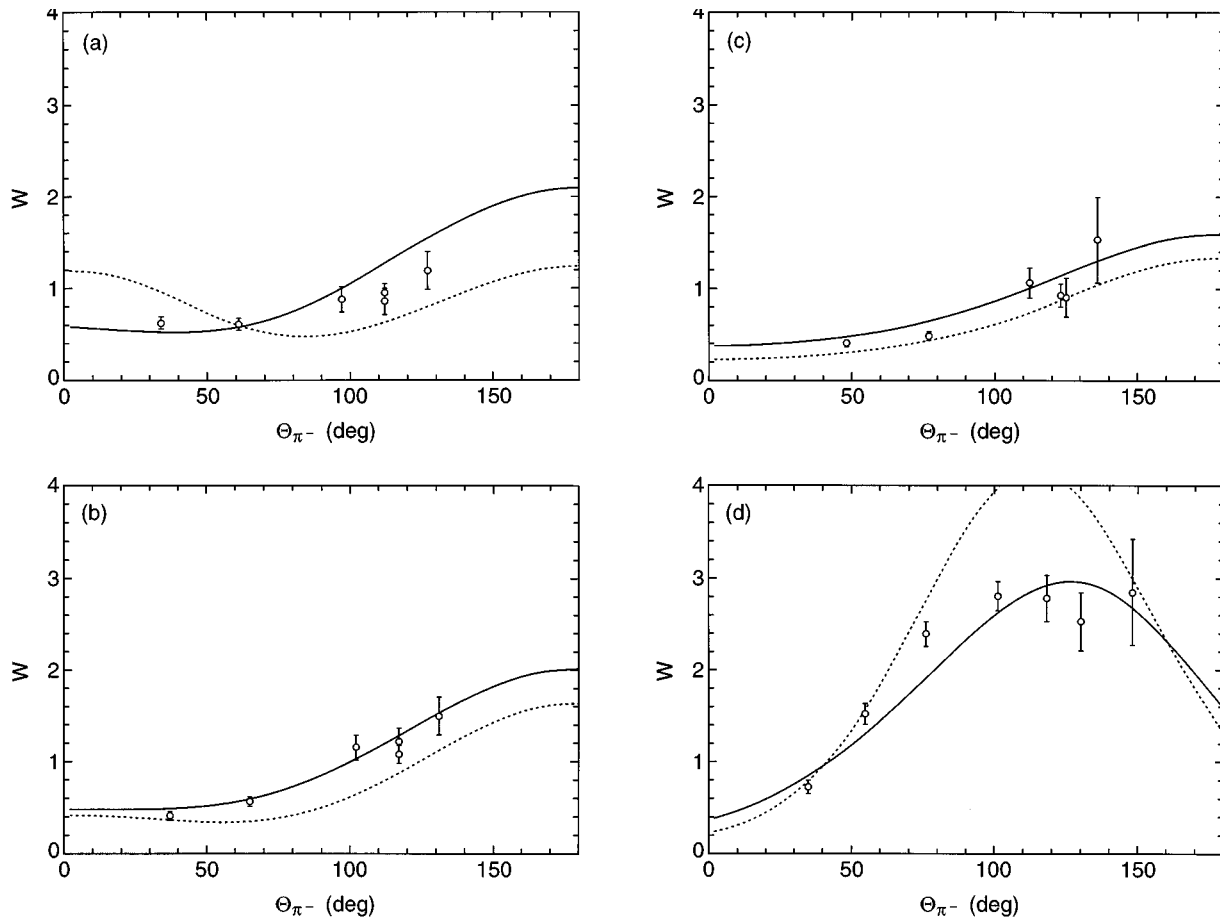
FIG. 7. The c.m. angular correlation function W for the reaction III. The ingoing π^- momentum defines the positive z axis; the figures show our results for various values of the outgoing π^+ momentum k_{π^+} and polar angles $\theta_{\pi^+}, \varphi_{\pi^+}$ as function of the outgoing π^- polar angles $\theta_{\pi^-}, \varphi_{\pi^-}$: (a) The experimental data is given for $k_{\pi^+} = (37\text{--}84 \text{ MeV}/c)$, $\theta_{\pi^+} = 91° \pm 10°$ and $\varphi_{\pi^-} = (85° - 95°)$; the figure shows our result for $k_{\pi^+} = 60 \text{ MeV}/c$, $\theta_{\pi^+} = 91°$, $\varphi_{\pi^+} = 0$, $\varphi_{\pi^-} = 90°$: —— with Δ and N^*; - - - - without Δ and N^*; $\bigcirc$ [20]; (b) Results for $k_{\pi^+} = 113 \text{ MeV}/c$, $\theta_{\pi^+} = 71°$ and $\varphi_{\phi^-} = 92°$. The experimental data is for $k_{\pi^+} = (102\text{--}124 \text{ MeV}/c)$, $\theta_{\pi^+} = 71° \pm 10°$; $\varphi_{\pi^-} = (85° - 95°)$; —— with Δ and N^*; - - - - without Δ and N^*; $\bigcirc$ [20]; (c) Results for $k_{\pi^+} = 152 \text{ MeV}/c$, $\theta_{\pi^+} = 67°$ and $\varphi_{\pi^-} = 92°$. The experimental data is for $k_{\pi^+} = (129\text{--}174 \text{ MeV}/c)$, $\theta_{\pi^+} = 67° \pm 10°$ and $\varphi_{\pi^-} = (85° - 96°)$; —— with Δ and N^*; - - - - without Δ and N^*; $\bigcirc$ [20]; (d) Results for $k_{\pi^+} = 152 \text{ MeV}/c$, $\theta_{\pi^+} = 67°$ and $\varphi_{\pi^-} = 92°$. The experimental data is for $k_{\pi^+} = (129\text{--}174 \text{ MeV}/c)$, $\theta_{\pi^+} = 67° \pm 10°$ and $\varphi_{\pi^-} = (85° - 96°)$; —— with Δ and N^*; - - - - without Δ and N^*; $\bigcirc$ [20].

We could force agreement (especially for A^{32}) if we also changed our other key parameters, first and foremost F and g_A.

Another piece of available data provides information on the invariant mass distributions $d\sigma/dm_{\pi\pi}$ and $d\sigma/dm_{\pi n}$.

1. $\pi° \pi°$

The most precise low energy results [17] give the $\pi° \pi°$ invariant mass distribution in reaction IV for kinetic energies between 168 and 280 MeV. In Fig. 8(a) we show a sample of our results at 230 and 300 MeV. We see that they qualitatively reproduce the experimentally observed trend favoring higher $m_{\pi\pi}$ masses relative to the phase space contribution.

2. $\pi^+ \pi^+$

Reaction I is used. For kinetic energies under 264 MeV, one finds just the phase space contribution, but for higher energies one sees [24] that lower masses $m_{\pi^+\pi^+}$ begin to be favored. Our calculations reproduce these trends.

3. $\pi^+ \pi°$ and $\pi^- \pi°$

These distributions can be measured from reaction II (between 189 and 260 MeV) [22] and reaction V [25], respectively. The experimental results for $\pi^- \pi°$ are essentially in agreement with pure phase space distributions: we calculated this mass distribution at 230 and 300 MeV, and basically found phase space distributions, too.

The experimental results for $\pi^+ \pi°$ between 189 and 260 MeV essentially show phase space distributions. Our calculations again refer to 230 and 300 MeV, but we do find a noticeable trend favoring higher invariant masses, when the calculated distributions are divided by the phase space contribution. However, the results of Phŏcanič et al. [22] did not register this effect.

4. $\pi^+ \pi^-$

The data comes from reaction III at 284 MeV [20] and at 332 MeV [26]. These experiments clearly show preference for higher invariant masses. Our calculation, done at 230 and 300 MeV, agrees with this observation.
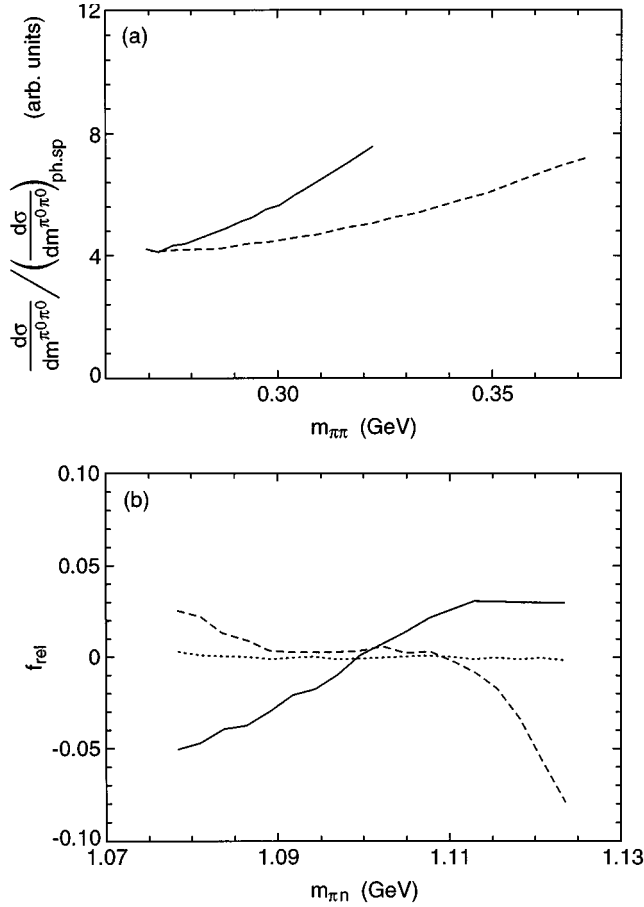
FIG. 8. (a) The invariant $\pi^{\circ}\pi^{\circ}$-mass distribution for reaction IV divided by the phase space contribution; —— $T = 230$ MeV, - - - - $T = 300$ MeV; (b) The asymmetry parameter for the $(\pi^{\pm}n)$ mass distribution for reaction III at 230 MeV; —— with Δ and N^*; - - - - without Δ and N^*; $\cdots\cdots$ phase space contribution.

5. $\pi^- n$ and $\pi^+ n$

Experiments using Reaction III (at 298 MeV) [27] and higher energies show that there is an asymmetry in the invariant mass distributions of the pair $\pi^- n$ and the pair $\pi^+ n$: $\pi^+ n$ shows preference for lower invariant masses in contrast to $\pi^- n$.

In order to investigate this, we calculate the asymmetry parameter

$$f_{\text{rel}}(m_{\pi n}) \equiv \frac{(d\sigma/dm_{\pi^- n}) - (d\sigma/dm_{\pi^+ n})}{(d\sigma/dm_{\pi^- n}) + (d\sigma/dm_{\pi^+ n})}.$$

Our results, shown in Fig. 8(b), are in qualitative agreement with the data. One can clearly see the influence of the baryonic resonances on this asymmetry effect.

Summarizing, we conclude the following. As expected, BχPTh is at its best at relatively low energies above thresholds. Thus there is a reasonable agreement with the experimental data on cross sections, angular distributions and invariant mass distributions, and this for pion kinetic energies up to about 120 MeV above their threshold values. No parameter fitting to this data was attempted and all the relevant key parameters introduced by BχPTh are already more or
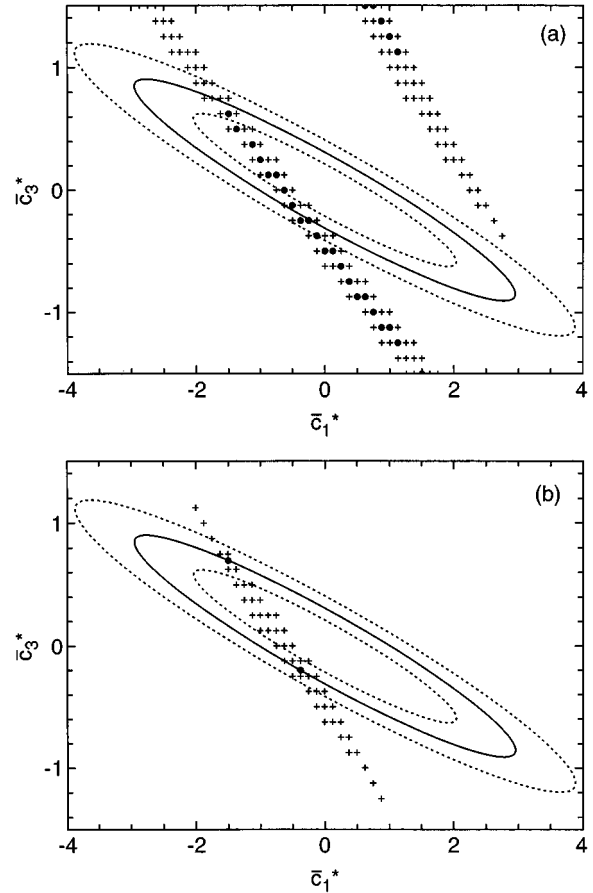
FIG. 9. The $(\bar{c}_1^*, \bar{c}_3^*)$ plane showing the elliptical band within which agreement with the data on N^* decays can be obtained; (a) The $\bullet$ and $+$ show the points in this plane where agreement with the experimental angular distributions for reaction III at 203 MeV can also be obtained: $\bullet$ the rms division R (Sec. IV) is "good," i.e., around $(-1.5, 0.7)$ and $(-0.37, -0.20)$; $+$ R is "poor/fair"; At 230 MeV, only the second region is still "good." (b) The $(\bar{c}_1^*, \bar{c}_3^*)$ plane: ($\bullet$) indicates $(-1.5, 0.7)$ and $(-0.37, -0.20)$; $(+)$ stands for values leading to $R < 2$ for both the differential cross section for channel (III) at 203 MeV and total cross section for channel (IV) under 200 MeV [17]. Taking further into account the final state $(\pi\pi)$ invariant mass distributions, the region $(-0.37, -0.20)$ is preferred, using energy-dependent N^* and Δ linewidths. For energy independent linewidths this changes to $(-0.72, -0.09)$.

less fixed by independent data. In fact, we used these results to further restrain the parameter space of the N^* decay [Figs. 9(a) and 9(b)]. The correct inclusion of baryonic resonances may or may not be important. For $\pi^+ p \to \pi^+ \pi^+ n$, neither Δ nor N^* are important; for $\pi^{\pm} p \to \pi^{\circ} \pi^{\pm} p$ Δ is very important, but N^* is not important; for the $\pi^- p \to \pi^+ \pi^- n$ reaction N^* is very important, Δ is important; and finally for the $\pi^- p \to \pi^{\circ} \pi^{\circ} n$ reaction, N^* is very important, whereas the Δ is negligible. The correct choice of the linewidths at the relevant energies for these baryonic resonances plays a very important role, in that the results are sensitive to the prescription used. Comparisons of our results to the findings of Müller *et al.* [20] on W show rather poor quantitative agreement, in general. Trends in the invariant mass distributions of the final pion pair, or the $\pi^{\pm} n$ pair are in qualitative agreement with the data; they clearly reproduce deviations

from pure phase space distributions, if such exist at the energies considered.

ACKNOWLEDGMENTS

We should like to express our thanks to Geoff Oades for his friendly advice, suggestions and encouragement, and to J. Beringer for his kind permission to use his computer code PHYSICA which made the initiation of this work possible.

APPENDIX

We shall here discuss how the low-energy data on $\pi N \rightarrow \pi\pi N$ could be of help in fixing the parameters $\bar{c}_1^*$ and $\bar{c}_3^*$ introduced in Sec. II and in principle allowed by the rules of BχPTh. This is feasible, because processes such as $\pi^- p \rightarrow \pi^+ \pi^- n$ and $\pi^- p \rightarrow \pi^\circ \pi^\circ n$ have calculated rates that turn out to be sensitive to $\bar{c}_1^*$ and/or $\bar{c}_3^*$.

Our primary source of information [2] is the linewidth and BR for the strong $N^* \rightarrow N\pi$ and $N^* \rightarrow N\pi\pi$ decays. Unfortunately, there is a considerable amount of uncertainty regarding these data [2]. Thus the relevant width $\Gamma_{N(\pi\pi)_{I=0}}$ is assumed to be only about 5–10 % of Γ_{N*}, whereas the BR for $N^* \rightarrow N\pi$ is about 60–70 %. We took as central values 7.5 and 65 %, respectively. The procedure is to calculate the rms deviation

$$R = \sqrt{\frac{1}{N}\sum_{i=1}^{N}\left[\frac{f_i(\text{teo}) - f_i(\text{exp})}{\Delta f_i(\text{exp})}\right]^2},$$

where $f_i(\text{exp})$, $\Delta f_i(\text{exp})$, and $f_i(\text{teo})$, respectively, are the central value and the uncertainty of the experimental quantity f_i, and its calculated theoretical value. We consider $R < 1$ to be ''good agreement'' (denoted in the figures by

●), whereas $1 < R < 2$ is considered ''poor/fair agreement'' (denoted in the figures by $+$). The measured quantities used were: (1) $d^3\sigma/d\Omega dT$ from Manley *et al.* at 203 MeV and 230 MeV for $\pi^- p \rightarrow \pi^+ \pi^- n$ [28]; (2) Total cross section for $\pi^- p \rightarrow \pi^\circ \pi^\circ n$ for kinetic energies less than 200 MeV, i.e., for under about 40 MeV over threshold (the first ten measured values from Lowe *et al.* [17]); (3) Invariant mass distributions for the $\pi^\circ \pi^\circ$ pair produced in the reaction $\pi^- p \rightarrow \pi^\circ \pi^\circ n$ at kinetic energies from 168 to 280 MeV [17].

Figs. 9(a) and 9(b) illustrate our results. Perusal of these figures shows that (1) There are clearly two regions in the $(\bar{c}_1^*, \bar{c}_3^*)$ plane where some set of observables mentioned above [i.e., (1) and (2)] are rather well reproduced by our calculations; they are centered around $(-1.5, 0.7)$ and $(-0.37, -0.20)$; (2) A clear preference emerged for the region around $(-0.37, -0.20)$ when *all* the calculations for observables reported in this paper were repeated; (3) The alternative region mentioned above, viz., $(-1.5, 0.7)$ is also unfavored by (3), as it leads to disagreement with the experimentally observed preference for higher invariant masses.

We must note, however, that these results are somewhat sensitive not only to the values of the BR but especially to the assumed energy dependence of the linewidths. We recall that all the hitherto discussed results in this Appendix refer to the choice Γ_2 (energy-dependent linewidth introduced in the main text). It turns out that if instead we use energy-independent linewidths (also discussed in the main text), the result is a slight change in the allowed parameter space: from $(-0.37, -0.20)$ to $(-0.72, -0.09)$, and from $(-1.50, 0.70)$ to $(-1.82, 0.76)$. The first mentioned new region is still the one, however, which leads to a more satisfactory agreement with all the available data.

[1] J. Bjorken and S. Drell, *Relativistic Quantum Fields* (McGraw Hill, New York, 1965), p. 377.

[2] Particle Data Group, Phys. Rev. D **50**, 1173 (1994).

[3] J. Beringer, πN Newsletter **7**, 33 (1992).

[4] H. Georgi, *Weak Interactions and Modern Particle Theory* (Addison-Wesley, Reading, MA, 1984), p. 92.

[5] J. F. Donoghue, E. Golowich and B. R. Holstein, *Dynamics of the Standard Model* (Cambridge University Press, Cambridge, (1992), p. 97.

[6] Ulf-G. Meissner, Rep. Prog. Phys. **56**, 903 (1993).

[7] S. Weinberg, Phys. Rev. Lett. **18**, 168 (1967).

[8] R. D. Peccei, Phys. Rev. **176**, 1812 (1968).

[9] M. Benmerrouche, R. M. Davidson, and N. C. Mukhopadhyay, Phys. Rev. C **39**, 2339 (1989).

[10] T. Ericson and W. Weise, *Pions and Nuclei* (Clarendon Oxford, 1988).

[11] S. Huber and J. Aichelin, Nucl. Phys. **A573**, 587 (1994).

[12] E. Oset and M. J. Vicente Vacas, Nucl. Phys. **A446**, 584 (1985).

[13] V. Bernard, N. Kaiser and Ulf-G. Meissner, Phys. Lett. B **309**, 421 (1993).

[14] O. Jäkel, H. W. Ortner, M. Dillig and C. Z. Vasconcellos,

Nucl. Phys. **A511**, 733 (1990); O. Jäkel, M. Dillig and C. A. Z. Vasconcellos, *ibid.* **A541**, 675 (1992); O. Jäkel and M. Dillig, *ibid.* **561**, 557 (1993).

[15] J. A. Gomez Tejedor and E. Oset, Nucl. Phys. **A571**, 667 (1994).

[16] V. Sossi *et al.*, Nucl. Phys. **A548**, 562 (1992).

[17] J. Lowe *et al.*, Phys. Rev. C **44**, 956 (1991).

[18] J. Lowe and H. Burkhardt, πN Newsletter **6**, 121 (1992).

[19] Ulf-G. Meissner (private communication).

[20] R. Müller *et al.*, Phys. Rev. C **48**, 981 (1993).

[21] H. Burkhardt and J. Lowe, Phys. Rev. Lett. **67**, 2622 (1991); πN Newsletter **8**, 174 (1993).

[22] D. Pǒcanić *et al.*, Phys. Rev. Lett. **72**, 1156 (1994)

[23] V. Bernard, N. Kaiser and Ulf-G. Meissner, Nucl. Phys. **B457**, 147 (1995).

[24] OMICRON Collaboration, Z. Phys. C **48**, 201 (1990).

[25] OMICRON Collaboration, Phys. Lett. B **225**, 198 (1989).

[26] OMICRON Collaboration, Phys. Lett. B **216**, 244 (1989).

[27] J. A. Jones, W. W. Allison and D. H. Saxon, Nucl. Phys. **B83**, 93 (1974).

[28] D. M. Manley, Phys. Rev. D **30**, 536 (1984).

[29] M. E. Sevior *et al.*, Phys. Rev. Lett. **66**, 2569 (1991).

[30] A. V. Kravtsov, A. V. Kuptsov, L. L. Nemenov, E. A. Starch-enko, D. M. Khazins, Sov. J. Nucl. Phys. **20**, 500 (1975).

[31] Yu. A. Batusov, S. A. Bunyatov, G. R. Gulkanyan, V. M. Sidorov, M. Musakhanov, G. Ionice, E. Losnianu, V. Mihul, D. Tuvdendorzh, Sov. J. Nucl. Phys. **21**, 162 (1975).

[32] M. Arman, D. J. Blasberg, R. P. Haddock, K. C. Leung, B. M. K. Nefkens, B. L. Schrock, D. I. Sober and J. M. Sperinde, Phys. Rev. Lett. **29**, 962 (1972).

[33] V. E. Barnes *et al.*, CERN Report No. 63-27 (1963).

[34] C. W. Bjork *et al.*, Phys. Rev. Lett. **44**, 62 (1980).

[35] I. M. Blair, H. Müller, G. Torelli, E. Zavattini, and G. Man-drioli, Phys. Lett. B **32**, 528 (1970).

[36] A. A. Bel'kov, S. A. Bunyatov, B. Zh. Zalikhanov, V. S. Kurbatov, A. Khalbaev, V. A. Yarba, Sov. J. Nucl. Phys. **31**, 96 (1980).

[37] A. A. Bel'kov, S. A. Bunyatov, B. Zh Zalikhanov, V. S. Kurbatov, A. Khalbaev, Sov. J. Nucl. Phys. **28**, 657 (1978).

[38] S. A. Bunyatov, G. V. Zholobov, B. Zh. Zalikhanov, V. S. Kurbatov, M. M. Musakhanov, A. Khalbaev, V. A. Yarba, Sov. J. Nucl. Phys. **25**, 177 (1977).

[39] D. H. Saxon, J. H. Mulrey and W. Chinowsky, Phys. Rev. D **2**, 1790 (1970).